Published in final edited form as:
Biomaterials. 2012 October ; 33(28): 6823–6832. doi:10.1016/j.biomaterials.2012.06.003.

Controlled Release of Dexamethasone from Peptide Nanofiber Gels to Modulate Inflammatory Response

Matthew J. Webber, PhD[^],
Northwestern University, Biomedical Engineering Department, Evanston, IL 60208

John B. Matson, PhD[^],
Northwestern University, Institute for BioNanotechnology in Medicine, Chicago, IL 60611

Vibha K. Tamboli, and
Northwestern University, Master of Biotechnology Program, Department of Chemical and Biological Engineering, Evanston, IL 60208

Samuel I. Stupp, Ph.D.[*]
Department of Materials Science and Engineering, Department of Chemistry, Evanston, IL 60208

Department of Medicine, Institute for BioNanotechnology in Medicine, Chicago, IL 60611

Abstract

New biomaterials that have the ability to locally suppress an immune response could have broad therapeutic use in the treatment of diseases characterized by acute or chronic inflammation or as a strategy to facilitate improved efficacy in cell or tissue transplantation. We report here on the preparation of a modular peptide amphiphile (PA) capable of releasing an anti-inflammatory drug, dexamethasone (Dex), by conjugation via a labile hydrazone linkage. This molecule self-assembled in water into long supramolecular nanofibers when mixed with a similar PA lacking the drug conjugate, and the addition of calcium salt to screen electrostatic repulsion between nanofibers promoted gel formation. These nanofiber gels demonstrated sustained release of soluble Dex for over one month in physiologic media. The Dex released from these gels maintained its anti-inflammatory activity when evaluated in vitro using a human inflammatory reporter cell line and furthermore preserved cardiomyocytes viability upon induced oxidative stress. The ability of this gel to mitigate the inflammatory response in cell transplantation strategies was evaluated using cell-surrogate polystyrene microparticles suspended in the nanofiber gel that were then subcutaneously injected in a mouse. Live animal luminescence imaging using the chemiluminescent reporter molecule luminol showed a significant reduction in inflammation at the site where particles were injected with Dex-PA compared to the site of injection for particles within a control PA in the same animal. Histological evidence suggested a marked reduction in the number of infiltrating inflammatory cells when particles were delivered within Dex-PA nanofiber gels and very little inflammation was observed at either 3 days or 21 days post-implantation. The use of Dex-PA could facilitate localized anti-inflammatory activity as a component of biomaterials designed for various applications in regenerative medicine and could specifically be a useful module for PA-based therapies. More broadly, these studies define a

[*]SIS- Person to whom correspondences should be addressed, Fax: (+1)847-491-3010, s-stupp@northwestern.edu.
[^]MJW and JBM contributed equally to this work

versatile strategy for facile synthesis of self-assembling peptide-based materials with the ability to control drug release.

Keywords

Inflammatory Response; Peptide Amphiphiles; Controlled drug release; Self-assembly; Immune response; Cell therapy

Introduction

One major challenge in the field of biomaterials is to develop strategies to combat the innate host inflammatory response [1, 2]. Many commonly used biomaterials, including collagen and alginate, elicit some cell-mediated immune response at the implantation site [3–7]. Though a mild innate immune response is part of the normal healing process following implantation of a foreign material, such a response could prove detrimental when combined with the delivery and transplantation of fragile cells, islets, or tissue [8–11]. Using biomaterials to deliver therapeutic cells adds additional factors that could influence the inflammatory response, including issues of cell source or transplant location. For example, strategies delivering autologous cells as therapy for cardiovascular disease have demonstrated limited efficacy, resulting in part from the enhanced inflammatory environment of ischemic tissue [12]. Islet transplantation to combat type 1 diabetes mellitus, meanwhile, relies on allogeneic (or even xenogeneic) tissue sources, which makes managing the inflammatory response paramount for effective therapy [11]. Strategies to combat immune-destruction of transplanted islets have included immunoisolation through encapsulation in biomaterials, but such strategies have demonstrated only limited success thus far as the construct size is often too big for injection and the encapsulation results in limitations to nutrient and oxygen transport [13–15]. The development of new materials that actively mitigate the local host immune response and facilitate improved efficacy in cell or tissue transplantation therefore remains an important objective.

One approach that has been used to modulate the host immune response is to design biomaterials with controlled release of anti-inflammatory drugs such as dexamethasone (Dex), a potent steroidal anti-inflammatory and immune response-suppressing drug [16]. In addition, Dex is known to be an important signaling molecule to promote differentiation in bone marrow-derived stromal cells and mesenchymal stem cells [17–21]. In order to harness its anti-inflammatory function or to stimulate differentiation, non-covalent Dex incorporation and release has been included in the design of a number of biomaterials [22–27]. Several constructs incorporating this drug have been evaluated *in vivo*, demonstrating a significant reduction in the post-implant inflammatory response to a material [28] and also promoting osteogenesis in transplanted stem cells when its release is combined into the delivery scaffold [29, 30]. In a few instances, biomaterials have been designed to control the release of Dex using covalent attachment via hydrolysable linkages, including hydrazones and lactide esters, which are labile in aqueous conditions to release the free drug [31–35].

Over the last decade, our group and others have investigated self-assembling peptide-based materials for applications in regenerative medicine, drug delivery, and cancer [36–46]. In particular, our group has focused on a class of molecules, termed peptide amphiphiles (PAs), which contain a short peptide sequence covalently attached to a saturated alkyl tail and self-assemble into fiber-like nanostructures [47, 48]. The assembly of these molecules occurs through hydrophobic collapse of their alkyl tails and hydrogen bonding leading to the formation of β-sheet structures near the core of the nanofiber [49, 50]. On the end opposite the hydrophobic tail, PAs can be synthesized to contain a bioactive peptide designed to

interact with biological targets such as cell receptors [51, 52], biopolymers [53, 54], or proteins [55]. In other systems, PAs can be integrated with commonly used biomaterials such as collagen or poly(L-lactic acid) [56, 57]. The conserved amphiphilic molecular design enables the modular construction of PA nanofibers that combine different PA molecules within the same assembled nanofiber as a way to multiplex different bioactivities or optimize the spacing of bioactive ligands [55, 58].

We report here the design, synthesis, and function of a PA that could allow controlled release of Dex through the use of a hydrazone linkage. While previous attempts to combine drug release with PA technology have focused on solubilizing hydrophobic drugs in the lipid core of the assembled fiber [59–61], this approach using covalent attachment via a hydrazone could facilitate enhanced control over the kinetics of drug release [62, 63]. A Dex-releasing PA (Dex-PA) could potentially be easily integrated with other bioactive PAs to therapeutically reduce or eliminate the immune response. In this work, a PA conjugated with Dex was synthesized and PA nanofiber gels were prepared that could release the soluble drug over a period of several weeks. Using in vitro methods, we evaluated the anti-inflammatory and cytoprotective activity of released Dex. Finally, an in vivo model was used to evaluate the ability of the Dex-PA to mitigate the inflammatory response to cell surrogate microparticles delivered within a Dex-PA nanofiber gel.

Materials and Methods

Dex-PA Synthesis

Rink Amide MBHA resin and Fmoc-protected amino acids were purchased from EMD. Dex was purchased from Spectrum and used as received. All solvents were ACS reagent grade and purchased from Mallinckrodt. Other peptide synthesis reagents were purchased from commercial sources and used as received. 1-[N, N, N'-Tris((*tert*-butyloxycarbonyl))hydrazide]-adipic acid ($HAA(Boc)_3$) was synthesized as previously described and used to synthesize a PA containing a free hydrazide, as also described previously, from Rink Amide MBHA resin using standard solid phase synthesis conditions [62]. Scheme 1 illustrates the process to synthesize a peptide with a free hydrazide using standard solid phase peptide synthesis methodology. For each amino acid coupling, 4 equiv. of Fmoc-protected amino acid was added using 4 equiv. HBTU and 6 equiv. DIEA in DMF (HBTU = O-benzotriazole-N,N,N’,N’-tetramethyluronium-hexafluorophosphate; DIEA = N,N-diisopropylethylamine; DMF=dimethylformamide). Fmoc removal was accomplished with 30% piperidine in DMF. For addition of $HAA(Boc)_3$, Fmoc-Lys(Mtt)-OH was added to the resin, and the Mtt group was removed on-resin by agitation in 4% TFA and 4% TIPS in CH_2Cl_2 (TFA = trifluoroacetic acid; TIPS = triisopropylsilane). The resin was briefly washed with 5% DIEA in DMF, then $HAA(Boc)_3$ (2.5 equiv) was added with 2.5 equiv HBTU and 4 equiv DIEA in DMF. The palmitic acid tail was added using the same conditions as the Fmoc-amino acids. The PA was cleaved from the resin using a peptide cleavage solution of 95% TFA, 2.5% TIPS and 2.5% H_2O. Concentration of the cleavage solution in vacuo and precipitation of the residue into cold Et_2O afforded the crude product, which was purified by preparative HPLC on a Varian Prostar 210 HPLC system, eluting with a gradient of 2% ACN to 100% ACN in water on a Phenomenex C18 Gemini NX column (150 × 30 mm) with 5 μm pore size and 110Å particle size. 0.1% NH_4OH was added to both mobile phases to aid PA solubility. Product-containing fractions were confirmed by ESI mass spectrometry (Agilent 6510 Q-TOF LC/MS), combined, and lyophilized after removing ACN by rotary evaporation. MS (M+H): calc’d: 1123.72; found: 1123.72. The control PA (sequence: C_{16}–$V_2A_2E_2$), which was also used to dilute the Dex-PA and facilitate nanofiber gel formation, was synthesized and purified by similar methods, as described previously [62].

Dex-PA was synthesized by condensation of hydrazide-PA with Dex. First, purified hydrazide-PA (35 mg) was taken up in TFA (400 μL) then precipitated with cold Et_2O (15 mL). The mixture was centrifuged and the solvent was removed. The solids were suspended again in Et_2O (15 mL) and centrifuged. After solvent removal the solids were dried under vacuum to constant mass. DMSO/MeOH (400 μL, 1:1 v/v) was added to the dried hydrazide-PA, followed by Dex (16 mg) and acetic acid (3 μL). The reaction mixture was sonicated at 50 °C for 1 h and then allowed to sit in a water bath at 50 °C overnight. A robust gel formed and was taken up in 3 mL hexafluoroisopropanol (HFIP) with stirring and sonication. The HFIP was then removed by rotary evaporation and the DMSO solution was taken up in 0.1% NH_4OH and purified by HPLC as described above. Product containing fractions were combined and lyophilized. MS (M+H): calc'd: 1497.91; found: 1497.92.

Structural Characterization

TEM samples were cast from 0.1 wt.% solutions in 2 mM NaOH onto carbon film on copper 300 mesh TEM grids (Electron Microscopy Sciences). Samples were then stained with a 2% solution of uranyl acetate in water. Images were taken on a JEOL 1230 TEM with an accelerating voltage of 100 kV using a Gatan 831 bottom-mounted camera.

Scanning electron microscopy (SEM) was performed using a Hitachi S4800 SEM with a 5 kV accelerating voltage. A 50 μl solution of a 1 wt.% Dex-PA/control PA mixture (1:9) was prepared and then gelled by the addition of 10 μl of a 50 mM $CaCl_2$ solution. The sample was fixed in 2% glutaraldehyde and 3% sucrose in PBS for 30 minutes at 4°C followed by sequential dehydration in ethanol. It was then dried at the critical point and coated in 8 nm osmium prior to imaging.

Drug Release Studies

A mixture of Dex-PA (157 μg) and control PA (C_{16}–$V_2A_2E_2$, 1418 μg) was prepared by mixing both PAs from stock solutions in HFIP at 10 mg/mL. Lyophilization of the HFIP solution on a Schlenk line afforded a white powder containing 10% Dex-PA. The powder was taken up in 10 mM NaOH (157.5 μL) and divided into 6 aliquots of 25 μL each in Eppendorf tubes. Each solution was individually gelled with 5 μL $CaCl_2$ (50 mM) and allowed to stand overnight at room temperature. 150 μL PBS was added on top of each gel and the tubes were sealed and stored at 37 °C. At each timepoint, the entire release solution was removed and replaced with fresh PBS. No degradation of the gel was apparent over the course of the study. A physical mixture control was also prepared by identical methods except that in this group soluble Dex at an amount equivalent to that used in the Dex-PA group was mixed with a 10 mg/mL solution of the control PA. Dex content in the release media was quantified by measuring absorbance at 242 nm using an M5 Spectramax Plate Reader (Molecular Devices). The average of the 6 samples is shown, with error bars corresponding to the standard deviation of the cumulative release.

Inflammatory Cell Assays

For experiments involving THP-1 human monocytes, a NFκB reporter cell line designed to produce secreted embryonic alkaline phosphatase (SEAP) upon inflammatory activation was purchased from Invivogen (San Diego, CA). These cells were cultured in RPMI 1640 (2 mM L-glutamine, 1.5 g/L sodium bicarbonate, 4.5 g/L glucose, 10 mM HEPES and 1 mM sodium pyruvate) with 10% FBS (non-heat inactivated), 100 μg/mL Normacin, 1% Pen-Strep, and 200 μg/mL Zeocin. PA solutions at 1 wt.% of Dex-PA/control PA (1:9), control PA with an equivalent concentration of free Dex (physical mixture), and control PA alone were prepared in HFIP and lyophilized. PA solutions were then dissolved in Hank's balanced salt solution containing 10 mM NaOH. To prepare gels, 25 μL of PA was combined in a 96-well U-bottom plate with 5 μL of 50 mM $CaCl_2$. Cells were isolated from

culture, centrifuged, and resuspended in RPMI 1640 media with 10% heat inactivated FBS and no additional additives at 1.5 million cells/mL. To the U-bottom wells containing the PA gels, 200 μL of the cell suspension was added. This was followed by a 10 μL addition of 10 μg/mL *E. coli*-derived lipopolysaccharides (LPS) solution in PBS or 10 μL of PBS for the negative control wells. Plates were incubated for 24 hours at 37°C. After incubation, 20 μL of the media was collected from each well, placed into a flat-bottom 96-well plate, and mixed with 180 μL of Quanti-Blue ALP substrate (Invivogen). The plate was incubated at 37°C for two hours and absorbance was read at 635 nm on a standard plate reader. Absorbance values were normalized to control media and the inflammatory response was expressed as the normalized increase in SEAP activity as a fold-increase compared to this control. Two separate experiments were averaged for a total of N=14 for +LPS conditions and N=6 for –LPS conditions, with the difference in N owing to the baseline response in all groups in the absence of LPS.

Cardiomyocyte Oxidative Stress Assay

H9c2 cardiomyocytes were cultured in high glucose DMEM containing 10% heat-inactivated FBS and 1% penicillin/streptomycin. Cells were plated at 4,000/well in a 96-well plate and cultured overnight. The following day, media was exchanged for growth media containing 500 μM hydrogen peroxide and cells were cultured for two hours. Control cells were treated with growth media without hydrogen peroxide. Following the two-hour hydrogen peroxide exposure, media was removed and replaced with growth media for the controls or growth media supplemented with 1 μM Dex PA or free Dex. After 24 hours, an MTT assay was performed to quantify number of viable cells in each well. Briefly, 3-(4,5-dimethylthiazol-2-yl)-2,5-diphenyltetrazolium bromide (MTT) was dissolved at 500 μg/mL in growth media, 200 μL was added to each well, and the plate was incubated at 37°C for four hours. After this time, the media was removed and the plate was dried. Once dry, 200 μL of DMSO was added to each well; the plate was mixed for one hour, and absorbances of each well were read on a microplate reader at 570, with a background control wavelength of 630 nm. The absorbance of the untreated control condition was set to 100% and the readings for the remaining wells were scaled to this value. For imaging, a two-color Live/Dead stain (Invitrogen) was used to stain live cells with Calcein AM (green) and dead cells with ethidium homodimer (red).

Live Animal in vivo Imaging of Inflammatory Response

In order to evaluate the ability of the Dex-PA to suppress an immune response to transplanted cells, we used a subcutaneous implantation model in hairless SKH1-E mice (Charles River Laboratories, Inc). Unfunctionalized 20 μm polystyrene particles (Polysciences, Inc) were used as a cell surrogate and were chosen for their known capacity to promote an immune response [64]. The size was chosen to be on the order of a cell but also too large for macrophage endocytosis. Particles were washed 3 times in ethanol, with centrifugation and supernatant aspiration following each wash, and were finally rinsed once in saline to remove excess ethanol. The particle pellet was resuspended in a 1 wt.% solution of either the control PA or a 9:1 mixture of the control PA with Dex-PA at a final polystyrene particle content of approximately 13.7% by weight. The PA/particle solutions were injected subcutaneously into the flanks of anesthetized mice using a 50 μL syringe by filling the syringe first with 5 μL of a 1M $CaCl_2$ solution, followed by 25 μL of the PA/particle solution, and finally another 5 μL of the 1M $CaCl_2$ solution. Each animal received one injection of particles suspended in the control PA on the left flank and one injection of particles suspended in the 9:1 PA mixture containing Dex-PA on the right flank. To image the acute inflammatory response, we used live animal imaging on an IVIS Spectrum bioluminescence imager. At three days following implantation of materials, animals were anesthetized with isoflurane and administered an intraperitoneal injection of 5 mg luminol

sodium salt (Alfa Aesar) at 50 mg/mL. Mice were then transferred to the imaging chamber and were maintained on a plane of anesthesia using a nose-cone manifold for the duration of imaging. Luminol emits a photon of light as it reacts with reactive oxygen species, the production of which is a component of the inflammatory response. This experiment is commonly used to monitor the host inflammatory response to biomaterials by luminescence imaging [28, 65, 66]. Bioluminescence images with small binning and an exposure time of 3 minutes were collected and overlaid on a black and white photograph for aid in visualization. Prior to imaging, a marker was used to mark the skin of the animal for ease in locating the material in the images. Quantitative results were prepared from images collected 21 minutes after luminol injection, which corresponded to peak luminescent signal for these studies and is consistent with previous findings [66]. To quantify the inflammatory response, a circle (180 pixels in area) was drawn around the injection site of each material along with a representative background area using the accompanying IVIS Living Image 4.0 software package. Total flux (photons/second) was calculated for each region of interest, and background-subtracted values were generated from these quantities. In total, quantified data was obtained in 9 animals from two separate experiments conducted two weeks apart. One animal was not included in the quantification because of unexplained elevation in the background luminescence compared with the other 9 animals in the study. These studies were conducted under a protocol approved by the Northwestern ACUC.

Histological Evaluation

To corroborate findings from the *in vivo* imaging, half of the animals used for luminol-based detection of inflammatory response were sacrificed at 3 days and the other half were sacrificed at 21 days in order to view the response to the implanted materials at early and later time-points. Briefly, animals were sacrificed by CO_2 asphyxiation, and skin that contained the injected material adherent to its underside was isolated. Tissue was fixed in formalin for 3 days, following which it was processed by standard methods, embedded in paraffin, and sectioned. Sections were performed with the skin on-edge to view the interface between the material and skin and were taken at several points throughout the thickness of the material. Samples were stained with H&E and were evaluated using a standard upright histology microscope for any notable histological observations. Representative images from this evaluation were collected at 40× using a color camera mounted on the microscope.

Statistics and Data Analysis

Cell culture data were analyzed using a one way analysis of variance (ANOVA) with a Bonferroni multiple comparisons *post-hoc* test. Results from *in vivo* imaging were analyzed using a two-tailed Student's t-test with significance of $P<0.05$. Statistical analysis was performed with the aid of Graphpad InStat v3.1a.

Results and Discussion

PA Design and Characterization

The Dex-PA was designed to release free Dex over time in physiological conditions through the use of a hydrolysable hydrazone linkage. Briefly, tri-Boc-hydrazido adipic acid ($HAA(Boc)_3$) was synthesized as previously described [62] and added to a PA with the sequence $C_{16}–V_2A_2E_2K$ via the ε-amine of the lysine residue on resin after selective removal of an Mtt protecting group on the lysine. Following cleavage in 95% TFA, a stabile hydrazide was generated. After purification by HPLC, the hydrazide-containing PA was condensed with Dex in DMSO to form the hydrazone-linked drug through the ketone on Dex. The structure of the resulting hydrazone-linked Dex-PA is shown in Figure 1A. This procedure, outlined in Scheme 1, is readily amenable to the standard solid phase synthesis of PAs or other peptide-based materials, and could be broadly used to conjugate virtually any

ketone- or aldehyde-containing drug to any suitably derivatized peptide. The conjugated drug product was purified by HPLC to remove unreacted PA and excess Dex. Transmission electron microscopy (TEM) imaging showed that the pure Dex-PA assembled to form short nanofibers (Figure 1C). The bulky and hydrophobic Dex component on the hydrophilic end of the PA molecule likely prevents the pure Dex-PA from assembling into long nanofibers via the highly ordered molecular packing of traditional PA designs, such as that seen for the control PA (sequence: C_{16}–$V_2A_2E_2$, Figure 1B and 1D). However, when Dex-PA is diluted 1:9 by mixing with this control PA, the high aspect-ratio assembled nanofibers formed are consistent with typical PA nanofiber assemblies (Figure 1E). It is likely that mixing with the control PA enables the formation of supramolecular nanofibers with Dex conjugates spaced sufficiently for the PA molecules to pack and assemble into high aspect-ratio nanofibers. An important feature of PA nanofibers is their ability to form robust gels by charge screening. The Dex-PA, again mixed 1:9 with the control PA, is also able to form entangled nanofiber gel networks at 1 wt.% total PA under calcium ion screening conditions. Using scanning electron microscopy (Figure 2A), we could visualize bundles of nanofibers that become entangled to form a three-dimensional gel network. This finding of robust calcium-induced gelation is consistent with our experience with other PA nanofibers that contain glutamic acids as solubilizing groups. It should be noted that here a simple control PA was mixed with Dex-PA but it is envisioned that the Dex-PA could be similarly mixed with other PA molecules containing specific bioactive epitopes for use in therapeutic applications.

Dex Release From PA Nanofiber Gels

The Dex-PA could be a useful component in PA nanofiber therapy by enabling the creation of peptide nanofiber gels with controlled release of soluble Dex. Accordingly, nanofiber gels prepared with the control PA at the same composition used for SEM studies were formed in order to probe drug release kinetics of the hydrolytically labile Dex from the Dex-PA. Gels were incubated at 37°C in a release buffer (pH 7.4), which was collected and replaced with fresh buffer every 2 days for about one month. The absorbance of the collected buffer was measured at 242 nm and compared to a standard curve of Dex in order to determine the percent of the total Dex amount released over time. Though hydrazone bonds are more prone to hydrolysis in acidic environments, we studied release at physiologic pH to mimic the condtions the PA will be exposed to in vivo. As shown (Figure 2B), the Dex PA gels displayed minimal burst release and zero-order release kinetics with sustained release over this 32-day study. By the end of this time, approximately 40% of the total Dex was released from these gels and no visible change in the gel was observed. As expected, free Dex mixed with the control PA demonstrated a greater burst release at the initial timepoint, and also had a faster release profile. While the physical mixture gel also released Dex for the entirety of the study, over 50% had released after just 5 days. The prolonged release from the Dex-PA gels validates the use of the hydrazone linkage to achieve prolonged Dex release at a steady rate. The Dex-PA nanofiber gels could therefore be useful to deliver a low and consistent dose of Dex for prolonged times, and indicates that these materials could have the release profile necessary for long-term localized anti-inflammatory activity. This strategy to use a hydrazone to control drug release kinetics could also be amenable to incorporation into the molecular design and solid-phase synthesis of many other classes of self-assembling peptide gelators [41, 67–69].

Anti-inflammatory Activity in vitro

As previously mentioned, Dex is a potent anti-inflammatory and immunomodulating drug that has been broadly applied in a number biomaterial strategies to mitigate immune response [22–27]. The Dex-PA has potential use as an injectable material for the localized and controlled release of Dex at a specific site owing to the increased retention in tissue of a PA nanofiber compared to the soluble drug. Moreover, the controlled release kinetics of the

hydrazone linkage allow for prolonged release of Dex for over one month. In order to evaluate whether Dex released from the PA was active and able to function in an anti-inflammatory manner, we used a THP-1 human monocyte cell line engineered to produce SEAP upon activation of NF-κB. The THP-1 cell line has a number of pattern-recognition receptors, including toll-like receptors (TLRs), which are activated in the presence of a recognized antigen, resulting in the onset of inflammatory signaling by NF-κB [70]. Because these cells have been engineered to produce and excrete SEAP upon NF-κB activation, the media of these cells can be isolated and assayed for its SEAP content using a colorimetric alkaline phosphatase assay. In this experiment, PA gels were prepared at 1 wt. % PA from a 1:9 solution of Dex PA mixed with the control PA, as was used in the release experiments. One control group was prepared containing only the gelled control PA mixed with unbound Dex in an amount equivalent to that used for the Dex-PA group. As a Dex-free control, a control PA gel alone was used. The non-adherent THP-1 cells were cultured in wells containing the gels and were stimulated with LPS derived from *E. coli,* which is known to be a potent TLR-4 agonist [71]. After 24 hours, the excreted SEAP content in the media was determined using a colorimetric assay. The SEAP content for media where cells were cultured with PA gels alone without LPS stimulation was indistinguishable from cell-free media controls, indicating that none of the PA gels promoted an NF-κB-linked inflammatory response from the cultured cells in the absence of LPS and, further, suggesting no evidence of cytotoxicity or induction of THP-1 inflammatory cascades by the PAs themselves (Figure 3). When LPS was added to stimulate an immune response, cells cultured in the presence of the control PA gel showed a 7.4 fold increase in SEAP production compared to LPS-free controls. Meanwhile, cells cultured in the presence of Dex-PA gels (4.7 fold, $P<0.001$) as well as gels produced with a physical mixture of Dex in the control PA (*5.6 fold,* $P<0.01$) showed a significant reduction in SEAP levels, suggesting a decrease in LPS-induced NF-κB activation. Differences between the Dex-PA gel group and the Dex physical mixture group were not significant, indicating that the amount of Dex made available from the Dex-PA was sufficient to suppress the inflammatory response. These data demonstrate that free Dex released from the Dex-PA maintains its anti-inflammatory bioactivity and confirm results obtained from the same cell line demonstrating the anti-inflammatory effects of Dex in the presence of LPS stimulation [72]. In order to amplify the anti-inflammatory effect observed, multiple signaling pathways could be affected through combination of Dex-PA with PA-based delivery of other anti-inflammatory drugs using a similar hydrazone strategy or in combination with anti-inflammatory gasotransmitters such and carbon monoxide, which we have recently demonstrated can be released from PAs modified to contain a ruthenium CO donor [73].

The pathology of many diseases can be made more severe as a result of both acute and chronic inflammation in tissue. For example, the pro-inflammatory environment in the ischemic myocardium can promote necrosis and apoptosis of myocardial tissue and facilitate the formation of a non-contractile fibrotic scar [74–76]. In order to evaluate the potential for the Dex-PA to reduce tissue damage resulting from ischemia-linked oxidative stress, we used a common in vitro model to study cardiomyocyte apoptosis by culture with hydrogen peroxide (H_2O_2), which is a representative reactive oxygen species [77, 78]. H9c2 cardiomyocytes were first stressed with H_2O_2 and were subsequently treated with Dex-PA or soluble free Dex (Figure 4). Otherwise untreated cardiomyocytes exposed to hydrogen peroxide showed a viability of approximately 61% relative to a healthy control (assumed 100%). When Dex-PA was added following hydrogen peroxide treatment, viability was significantly improved, resulting in approximately 78% ($P<0.001$ compared to controls) of cells remaining viable. The same was seen for the addition of soluble Dex, which significantly improved viability to approximately 83% ($P<0.001$ compared to controls). There was no significant difference between treatment with Dex PA and free Dex. However, if used in vivo, it is presumed that the delivery of Dex using the Dex-PA would provide a

more localized and tissue specific drug release than delivery of the freely diffusible drug. We have previously explored PA-based growth factor delivery to treat myocardial ischemia [79], and the addition of the Dex-PA module to such an approach could facilitate reduced myocardial scarring and improved hemodynamic function. Other strategies being explored to treat cardiovascular disease include PA delivery of therapeutic bone marrow-derived cell populations, which are known to have reduced viability as a result of the pro-inflammatory environment of ischemic tissue [52]. In the context of the results presented here, the Dex-PA could be a useful component for incorporation into injectable PA-based therapies designed to treat ischemic tissue in the myocardium or peripheral circulation through the delivery of bioactive signals or therapeutic cells.

Anti-Inflammatory Activity in vivo

Biomaterial-based delivery of therapeutic cells or islets could benefit from a strategy to mitigate the host inflammatory response and to promote transplant survival and function. The anti-inflammatory properties of the Dex-PA, combined with its ability to form solid nanofiber gels, could therefore be useful to suppress the localized immune cell response without relying on systemic immune suppression. In order to evaluate whether the Dex-PA could be used as an injectable material capable of promoting localized immune suppression, we employed in vivo imaging methods that have allowed others to screen a number of biomaterials for cell-mediated inflammatory response in an array format within the same animal [28, 65, 66]. Polystyrene (PS) microparticles were used as a transplanted cell surrogate and were also used to stimulate an inflammatory response. These particles were delivered via subcutaneous syringe injection in a suspension of control PA (left flank) or a 1:9 mixture of Dex-PA with control PA (right flank) using an injection strategy to promote rapid calcium-induced gelation at the injection site. At 3 days post-implantation, luminol sodium salt was systemically administered. This technique enables the detection of reactive oxygen species, known to be part of an inflammatory response, when these species react with luminol resulting in the production of a detectable photon. As shown (Figure 5), PS microparticles delivered within the control PA resulted in a luminescent signal (62,500 photons/second) that was significantly greater ($P=0.001$) than that arising from PS particles delivered within the Dex-PA (7,600 photons/second). This effect can be visualized in the representative images overlaying the luminescent signal on a black and white image from several mice in the study. In each animal shown, the location at which particles were injected within the control PA gel showed a strong luminescent signal. However, delivery of PS particles within Dex-PA did not result in a luminescent signal that was visibly elevated compared to the background. This result is interesting considering the distance between the two injection sites is on the order of one centimeter, indicating that the immune suppression resulting from the release of free Dex from the Dex-PA is limited to the area of material injection. A similar finding has been reported with Dex-loaded PLGA microspheres, where a high degree of drug loading suppressed the inflammatory response in a neighboring control injection site but lower drug loading only suppressed the immune response at the local area of injection [28]. The ability of Dex-PA to locally suppress the immune response at only the injection site could be useful in cell or islet delivery approaches and could obviate the practice of systemic immune suppression in allogeneic transplant strategies.

In order to corroborate findings from live animal imaging, tissue was harvested and evaluated by histology at either 3 days or 21 days following injection. It was our intention that the 3 day timepoint would allow us to view the acute inflammatory response concomitant with the time-course of in vivo imaging while the 21 day samples would give insight into the immune response at longer times. Representative images are shown (Figure 6) from the tissue/material interface for PS particles delivered within a control PA gel as well as those delivered within a Dex-PA gel. At 3 days this interface showed extensive

immune cell infiltration when PS particles were delivered within the control PA. Evidence pointed to the development of some fibrotic tissue at the immediate interface, while a high density of infiltrating cells could be seen surrounding the PS spheres. However, tissue from the same animal of the implantation bed containing PS particles delivered within Dex-PA gels indicated only minimal infiltration of inflammatory cells. In this case, much of the staining in the interstitial area between PS particles is likely attributed to the PA gel, as PA materials are known to stain positively with eosin [7]. Also, the tissue/material interface showed no visible sign of inflammation or fibrosis and instead appeared to have a clean border between tissue and material. At 21 days the immune response in histology appeared very similar to the findings at 3 days. Though there was a notable decrease in the number of infiltrating cells for the control PA group at 21 days compared to the response at 3 days, there were still a large number of infiltrating immune cells and evidence of fibrotic tissue. There was also an apparent increase in the amount of matrix encasing the particles. Interestingly, at 21 days the inflammatory response to samples of PS particles delivered within Dex-PA appeared very similar to that at 3 days, with very few infiltrating cells and a clean material/tissue interface suggesting very little immune response to this material at longer timepoints following implantation. This finding is consistent with the prolonged release seen from our release studies and suggests that soluble Dex released from the PA may be suppressing the immune response to the PS particles both during the acute phase following implantation and over time. Taken together, the results from both in vivo imaging and conventional histology support our conclusion that the Dex-PA gel has the ability to provide localized anti-inflammatory activity and can be used as part of a therapeutic PA material to contribute immune suppression to the area of material or cell transplant.

Conclusions

We have described a peptide amphiphile conjugated covalently through a labile hydrazone bond to the steroidal anti-inflammatory drug dexamethasone. This material, along with similar drug-conjugated peptide amphiphiles, could be useful as gel networks to provide prolonged and localized drug delivery at the site of injection. In this work, we showed through in vitro studies the cytoprotective and anti-inflammatory properties of this material. Additionally, in vivo studies in mice demonstrated the capacity of this PA to greatly reduce the localized acute inflammatory response without systemic immune suppression. Such drug-conjugated peptide amphiphiles could also be co-assembled with other bioactive peptide amphiphiles to enable integrated multi-component therapies for the treatment of disease, including myocardial infarction, or as a component of cell-delivery systems and could extend to a number of other PA-based therapies. The synthetic strategy reported here could furthermore be generalized to other targets in regenerative medicine and also adapted to other peptide gelator systems as it is highly amenable to solid-phase peptide synthesis and can conceivably be used to conjugate any ketone- or aldehyde-containing drug to virtually any peptide-based material.

Acknowledgments

This work was supported by NIH grant number 5R01DE015920. JBM was supported by an NIH postdoctoral fellowship (1F32AR061955-01) and MJW was supported by the NIH through the Northwestern University Regenerative Medicine Training Program (5T90-DA022881). Additionally, support was provided through a Northwestern Feinberg School of Medicine Dixon Translational Research Stewardship Award. The authors also gratefully acknowledge helpful discussion with Prof. Dong Wang (University of Nebraska), Prof. Dinender Singla and Reetu Singla (University of Central Florida), and Tram Dang (MIT).

References

1. Williams DF. On the mechanisms of biocompatibility. Biomaterials. 2008; 29:2941–2953. [PubMed: 18440630]
2. Remes A, Williams DF. Immune response in biocompatibility. Biomaterials. 1992; 13:731–743. [PubMed: 1391394]
3. Anderson JM, Defife K, McNally A, Collier T, Jenney C. Monocyte, macrophage and foreign body giant cell interactions with molecularly engineered surfaces. J Mater Sci Mater Med. 1999; 10:579–588. [PubMed: 15347970]
4. Anderson JM, Rodriguez A, Chang DT. Foreign body reaction to biomaterials. Semin Immunol. 2008; 20:86–100. [PubMed: 18162407]
5. Ghanaati S, Schlee M, Webber MJ, Willershausen I, Barbeck M, Balic E, et al. Evaluation of the tissue reaction to a new bilayered collagen matrix in vivo and its translation to the clinic. Biomed Mater. 2011; 6 015010.
6. Ghanaati S, Willershausen I, Barbeck M, Unger RE, Joergens M, Sader RA, et al. Tissue reaction to sealing materials: different view at biocompatibility. Eur J Med Res. 2010; 15:483–492. [PubMed: 21159573]
7. Ghanaati S, Webber MJ, Unger RE, Orth C, Hulvat JF, Kiehna SE, et al. Dynamic in vivo biocompatibility of angiogenic peptide amphiphile nanofibers. Biomaterials. 2009; 30:6202–6212. [PubMed: 19683342]
8. Sittinger M, Hutmacher DW, Risbud MV. Current strategies for cell delivery in cartilage and bone regeneration. Curr Opin Biotechnol. 2004; 15:411–418. [PubMed: 15464370]
9. Nilsson B, Korsgren O, Lambris JD, Ekdahl KN. Can cells and biomaterials in therapeutic medicine be shielded from innate immune recognition? Trends Immunol. 2010; 31:32–38. [PubMed: 19836998]
10. Cooke MJ, Zahir T, Phillips SR, Shah DS, Athey D, Lakey JH, et al. Neural differentiation regulated by biomimetic surfaces presenting motifs of extracellular matrix proteins. J Biomed Mater Res A. 2010; 93:824–832. [PubMed: 19653304]
11. Gibly RF, Graham JG, Luo X, Lowe WL Jr, Hering BJ, Shea LD. Advancing islet transplantation: from engraftment to the immune response. Diabetologia. 2011; 54:2494–2505. [PubMed: 21830149]
12. Frantz S, Bauersachs J, Ertl G. Post-infarct remodelling: contribution of wound healing and inflammation. Cardiovasc Res. 2009; 81:474–481. [PubMed: 18977766]
13. O'Sullivan ES, Vegas A, Anderson DG, Weir GC. Islets Transplanted in Immunoisolation Devices: A Review of the Progress and the Challenges that Remain. Endocr Rev. 2011
14. Wilson JT, Chaikof EL. Challenges and emerging technologies in the immunoisolation of cells and tissues. Adv Drug Deliv Rev. 2008; 60:124–145. [PubMed: 18022728]
15. Zimmermann H, Shirley SG, Zimmermann U. Alginate-based encapsulation of cells: past, present, and future. Curr Diab Rep. 2007; 7:314–320. [PubMed: 17686410]
16. Franz S, Rammelt S, Scharnweber D, Simon JC. Immune responses to implants - a review of the implications for the design of immunomodulatory biomaterials. Biomaterials. 2011; 32:6692–6709. [PubMed: 21715002]
17. Hamidouche Z, Fromigue O, Nuber U, Vaudin P, Pages JC, Ebert R, et al. Autocrine fibroblast growth factor 18 mediates dexamethasone-induced osteogenic differentiation of murine mesenchymal stem cells. J Cell Physiol. 2010; 224:509–515. [PubMed: 20432451]
18. Hamidouche Z, Hay E, Vaudin P, Charbord P, Schule R, Marie PJ, et al. FHL2 mediates dexamethasone-induced mesenchymal cell differentiation into osteoblasts by activating Wnt/beta-catenin signaling-dependent Runx2 expression. FASEB J. 2008; 22:3813–3822. [PubMed: 18653765]
19. Pittenger MF, Mackay AM, Beck SC, Jaiswal RK, Douglas R, Mosca JD, et al. Multilineage potential of adult human mesenchymal stem cells. Science. 1999; 284:143–147. [PubMed: 10102814]

20. Pittenger MF, Mosca JD, McIntosh KR. Human mesenchymal stem cells: progenitor cells for cartilage, bone, fat and stroma. Curr Top Microbiol Immunol. 2000; 251:3–11. [PubMed: 11036752]
21. Pittenger MF. Mesenchymal stem cells from adult bone marrow. Methods Mol Biol. 2008; 449:27–44. [PubMed: 18370081]
22. Bhardwaj U, Burgess DJ. Physicochemical properties of extruded and non-extruded liposomes containing the hydrophobic drug dexamethasone. Int J Pharm. 2010; 388:181–189. [PubMed: 20079409]
23. Zolnik BS, Burgess DJ. Evaluation of in vivo-in vitro release of dexamethasone from PLGA microspheres. J Control Release. 2008; 127:137–145. [PubMed: 18282629]
24. Hickey T, Kreutzer D, Burgess DJ, Moussy F. In vivo evaluation of a dexamethasone/PLGA microsphere system designed to suppress the inflammatory tissue response to implantable medical devices. J Biomed Mater Res. 2002; 61:180–187. [PubMed: 12007197]
25. Hickey T, Kreutzer D, Burgess DJ, Moussy F. Dexamethasone/PLGA microspheres for continuous delivery of an anti-inflammatory drug for implantable medical devices. Biomaterials. 2002; 23:1649–1656. [PubMed: 11922468]
26. Wang Q, Wang J, Lu Q, Detamore MS, Berkland C. Injectable PLGA based colloidal gels for zero-order dexamethasone release in cranial defects. Biomaterials. 2010; 31:4980–4986. [PubMed: 20303585]
27. Ito T, Fraser IP, Yeo Y, Highley CB, Bellas E, Kohane DS. Anti-inflammatory function of an in situ cross-linkable conjugate hydrogel of hyaluronic acid and dexamethasone. Biomaterials. 2007; 28:1778–1786. [PubMed: 17204321]
28. Dang TT, Bratlie KM, Bogatyrev SR, Chen XY, Langer R, Anderson DG. Spatiotemporal effects of a controlled-release anti-inflammatory drug on the cellular dynamics of host response. Biomaterials. 2011; 32:4464–4470. [PubMed: 21429573]
29. Kim MS, Kim SK, Kim SH, Hyun H, Khang G, Lee HB. In vivo osteogenic differentiation of rat bone marrow stromal cells in thermosensitive MPEG-PCL diblock copolymer gels. Tissue Eng. 2006; 12:2863–2873. [PubMed: 17518655]
30. Kim H, Suh H, Jo SA, Kim HW, Lee JM, Kim EH, et al. In vivo bone formation by human marrow stromal cells in biodegradable scaffolds that release dexamethasone and ascorbate-2-phosphate. Biochem Biophys Res Commun. 2005; 332:1053–1060. [PubMed: 15922303]
31. Liu XM, Quan LD, Tian J, Laquer FC, Ciborowski P, Wang D. Syntheses of click PEG-dexamethasone conjugates for the treatment of rheumatoid arthritis. Biomacromolecules. 2010; 11:2621–2628. [PubMed: 20831200]
32. Liu XM, Quan LD, Tian J, Alnouti Y, Fu K, Thiele GM, et al. Synthesis and evaluation of a well-defined HPMA copolymer-dexamethasone conjugate for effective treatment of rheumatoid arthritis. Pharm Res. 2008; 25:2910–2919. [PubMed: 18649124]
33. Wang D, Miller SC, Liu XM, Anderson B, Wang XS, Goldring SR. Novel dexamethasone-HPMA copolymer conjugate and its potential application in treatment of rheumatoid arthritis. Arthritis Res Ther. 2007; 9:R2. [PubMed: 17233911]
34. Shi X, Wang Y, Varshney RR, Ren L, Gong Y, Wang DA. Microsphere-based drug releasing scaffolds for inducing osteogenesis of human mesenchymal stem cells in vitro. Eur J Pharm Sci. 2010; 39:59–67. [PubMed: 19895885]
35. Nuttelman CR, Tripodi MC, Anseth KS. Dexamethasone-functionalized gels induce osteogenic differentiation of encapsulated hMSCs. J Biomed Mater Res A. 2006; 76:183–195. [PubMed: 16265650]
36. Cui H, Webber MJ, Stupp SI. Self-assembly of peptide amphiphiles: from molecules to nanostructures to biomaterials. Biopolymers. 2010; 94:1–18. [PubMed: 20091874]
37. Webber MJ, Kessler JA, Stupp SI. Emerging peptide nanomedicine to regenerate tissues and organs. J Intern Med. 2010; 267:71–88. [PubMed: 20059645]
38. Matson JB, Zha RH, Stupp SI. Peptide Self-Assembly for Crafting Functional Biological Materials. Curr Opin Solid State Mater Sci. 2011; 15:225–235. [PubMed: 22125413]
39. Matson JB, Stupp SI. Self-assembling peptide scaffolds for regenerative medicine. Chem Commun. 2012; 48:26–33.

40. Collier JH, Rudra JS, Gasiorowski JZ, Jung JP. Multi-component extracellular matrices based on peptide self-assembly. Chem Soc Rev. 2010; 39:3413–3424. [PubMed: 20603663]
41. Jung JP, Gasiorowski JZ, Collier JH. Fibrillar peptide gels in biotechnology and biomedicine. Biopolymers. 2010; 94:49–59. [PubMed: 20091870]
42. Woolfson DN, Mahmoud ZN. More than just bare scaffolds: towards multi-component and decorated fibrous biomaterials. Chem Soc Rev. 2010; 39:3464–3479. [PubMed: 20676443]
43. Fallas JA, O'Leary LE, Hartgerink JD. Synthetic collagen mimics: self-assembly of homotrimers, heterotrimers and higher order structures. Chem Soc Rev. 2010; 39:3510–3527. [PubMed: 20676409]
44. Sargeant TD, Guler MO, Oppenheimer SM, Mata A, Satcher RL, Dunand DC, et al. Hybrid bone implants: self-assembly of peptide amphiphile nanofibers within porous titanium. Biomaterials. 2008; 29:161–171. [PubMed: 17936353]
45. Silva GA, Czeisler C, Niece KL, Beniash E, Harrington DA, Kessler JA, et al. Selective differentiation of neural progenitor cells by high-epitope density nanofibers. Science. 2004; 303:1352–1355. [PubMed: 14739465]
46. Stendahl JC, Wang LJ, Chow LW, Kaufman DB, Stupp SI. Growth factor delivery from self-assembling nanofibers to facilitate islet transplantation. Transplantation. 2008; 86:478–481. [PubMed: 18698254]
47. Hartgerink JD, Beniash E, Stupp SI. Self-assembly and mineralization of peptide-amphiphile nanofibers. Science. 2001; 294:1684–1688. [PubMed: 11721046]
48. Hartgerink JD, Beniash E, Stupp SI. Peptide-amphiphile nanofibers: a versatile scaffold for the preparation of self-assembling materials. Proc Natl Acad Sci U S A. 2002; 99:5133–5138. [PubMed: 11929981]
49. Velichko YS, Stupp SI, de la Cruz MO. Molecular simulation study of peptide amphiphile self-assembly. J Phys Chem B. 2008; 112:2326–2334. [PubMed: 18251531]
50. Pashuck ET, Cui H, Stupp SI. Tuning supramolecular rigidity of peptide fibers through molecular structure. J Am Chem Soc. 2010; 132:6041–6046. [PubMed: 20377229]
51. Webber MJ, Tongers J, Newcomb CJ, Marquardt KT, Bauersachs J, Losordo DW, et al. Supramolecular nanostructures that mimic VEGF as a strategy for ischemic tissue repair. Proc Natl Acad Sci U S A. 2011; 108:13438–13443. [PubMed: 21808036]
52. Webber MJ, Tongers J, Renault MA, Roncalli JG, Losordo DW, Stupp SI. Development of bioactive peptide amphiphiles for therapeutic cell delivery. Acta Biomater. 2010; 6:3–11. [PubMed: 19635599]
53. Rajangam K, Behanna HA, Hui MJ, Han X, Hulvat JF, Lomasney JW, et al. Heparin binding nanostructures to promote growth of blood vessels. Nano Lett. 2006; 6:2086–2090. [PubMed: 16968030]
54. Capito RM, Azevedo HS, Velichko YS, Mata A, Stupp SI. Self-assembly of large and small molecules into hierarchically ordered sacs and membranes. Science. 2008; 319:1812–1816. [PubMed: 18369143]
55. Shah RN, Shah NA, Del Rosario Lim MM, Hsieh C, Nuber G, Stupp SI. Supramolecular design of self-assembling nanofibers for cartilage regeneration. Proc Natl Acad Sci U S A. 2010; 107:3293–3298. [PubMed: 20133666]
56. Harrington DA, Cheng EY, Guler MO, Lee LK, Donovan JL, Claussen RC, et al. Branched peptide-amphiphiles as self-assembling coatings for tissue engineering scaffolds. J Biomed Mater Res A. 2006; 78:157–167. [PubMed: 16619254]
57. Sur S, Pashuck ET, Guler MO, Ito M, Stupp SI, Launey T. A hybrid nanofiber matrix to control the survival and maturation of brain neurons. Biomaterials. 2012; 33:545–555. [PubMed: 22018390]
58. Mata A, Geng Y, Henrikson KJ, Aparicio C, Stock SR, Satcher RL, et al. Bone regeneration mediated by biomimetic mineralization of a nanofiber matrix. Biomaterials. 2010; 31:6004–6012. [PubMed: 20472286]
59. Kapadia MR, Chow LW, Tsihlis ND, Ahanchi SS, Eng JW, Murar J, et al. Nitric oxide and nanotechnology: A novel approach to inhibit neointimal hyperplasia. J Vasc Surg. 2008; 47:173–182. [PubMed: 18178471]

60. Webber MJ, Newcomb CJ, Bitton R, Stupp SI. Switching of self-assembly in a peptide nanostructure with a specific enzyme. Soft Matter. 2011; 7:9665–9672. [PubMed: 22408645]
61. Soukasene S, Toft DJ, Moyer TJ, Lu H, Lee HK, Standley SM, et al. Antitumor activity of Peptide amphiphile nanofiber-encapsulated camptothecin. ACS Nano. 2011; 5:9113–9121. [PubMed: 22044255]
62. Matson JB, Stupp SI. Drug release from hydrazone-containing peptide amphiphiles. Chem Commun. 2011; 47:7962–7964.
63. Matson JB, Newcomb CJ, Bitton R, Stupp SI. Nanostructure-templated control of drug release from peptide amphiphile nanofiber gels. Soft Matter. 2012; 8:3586–3595.
64. Orsini AJ, Ingenito AC, Needle MA, DeBari VA. The neutrophil response to polystyrene microspheres bearing defined surface functional groups. Cell Biophys. 1987; 10:33–43. [PubMed: 2440577]
65. Ma M, Liu WF, Hill PS, Bratlie KM, Siegwart DJ, Chin J, et al. Development of cationic polymer coatings to regulate foreign-body responses. Adv Mater. 2011; 23:H189–H194. [PubMed: 21567481]
66. Liu WF, Ma M, Bratlie KM, Dang TT, Langer R, Anderson DG. Real-time in vivo detection of biomaterial-induced reactive oxygen species. Biomaterials. 2011; 32:1796–1801. [PubMed: 21146868]
67. Zhao X, Zhang S. Molecular designer self-assembling peptides. Chem Soc Rev. 2006; 35:1105–1110. [PubMed: 17057839]
68. Woolfson DN. Building fibrous biomaterials from alpha-helical and collagen-like coiled-coil peptides. Biopolymers. 2010; 94:118–127. [PubMed: 20091877]
69. Gao Y, Yang Z, Kuang Y, Ma ML, Li J, Zhao F, et al. Enzyme-instructed self-assembly of peptide derivatives to form nanofibers and hydrogels. Biopolymers. 2010; 94:19–31. [PubMed: 20091873]
70. Dev A, Iyer S, Razani B, Cheng G. NF-kappaB and innate immunity. Curr Top Microbiol Immunol. 2011; 349:115–143. [PubMed: 20848362]
71. Beutler B. Tlr4: central component of the sole mammalian LPS sensor. Curr Opin Immunol. 2000; 12:20–26. [PubMed: 10679411]
72. Kern JA, Lamb RJ, Reed JC, Daniele RP, Nowell PC. Dexamethasone inhibition of interleukin 1 beta production by human monocytes. Posttranscriptional mechanisms. J Clin Invest. 1988; 81:237–244. [PubMed: 3257219]
73. Matson JB, Webber MJ, Tamboli VK, Weber B, Stupp SI. A peptide-based material for therapeutic carbon monoxide delivery. Soft Matter. in press.
74. Frangogiannis NG. Chemokines in the ischemic myocardium: from inflammation to fibrosis. Inflamm Res. 2004; 53:585–595. [PubMed: 15693606]
75. Frangogiannis NG. The role of the chemokines in myocardial ischemia and reperfusion. Curr Vasc Pharmacol. 2004; 2:163–174. [PubMed: 15320517]
76. Frangogiannis NG, Smith CW, Entman ML. The inflammatory response in myocardial infarction. Cardiovasc Res. 2002; 53:31–47. [PubMed: 11744011]
77. Singla DK, Singla RD, Lamm S, Glass C. TGF-beta2 treatment enhances cytoprotective factors released from embryonic stem cells and inhibits apoptosis in infarcted myocardium. Am J Physiol Heart Circ Physiol. 2011; 300:H1442–H1450. [PubMed: 21297031]
78. Singla DK, McDonald DE. Factors released from embryonic stem cells inhibit apoptosis of H9c2 cells. Am J Physiol Heart Circ Physiol. 2007; 293:H1590–H1595. [PubMed: 17545477]
79. Webber MJ, Han X, Murthy SN, Rajangam K, Stupp SI, Lomasney JW. Capturing the stem cell paracrine effect using heparin-presenting nanofibres to treat cardiovascular diseases. J Tissue Eng Regen Med. 2010; 4:600–610. [PubMed: 20222010]

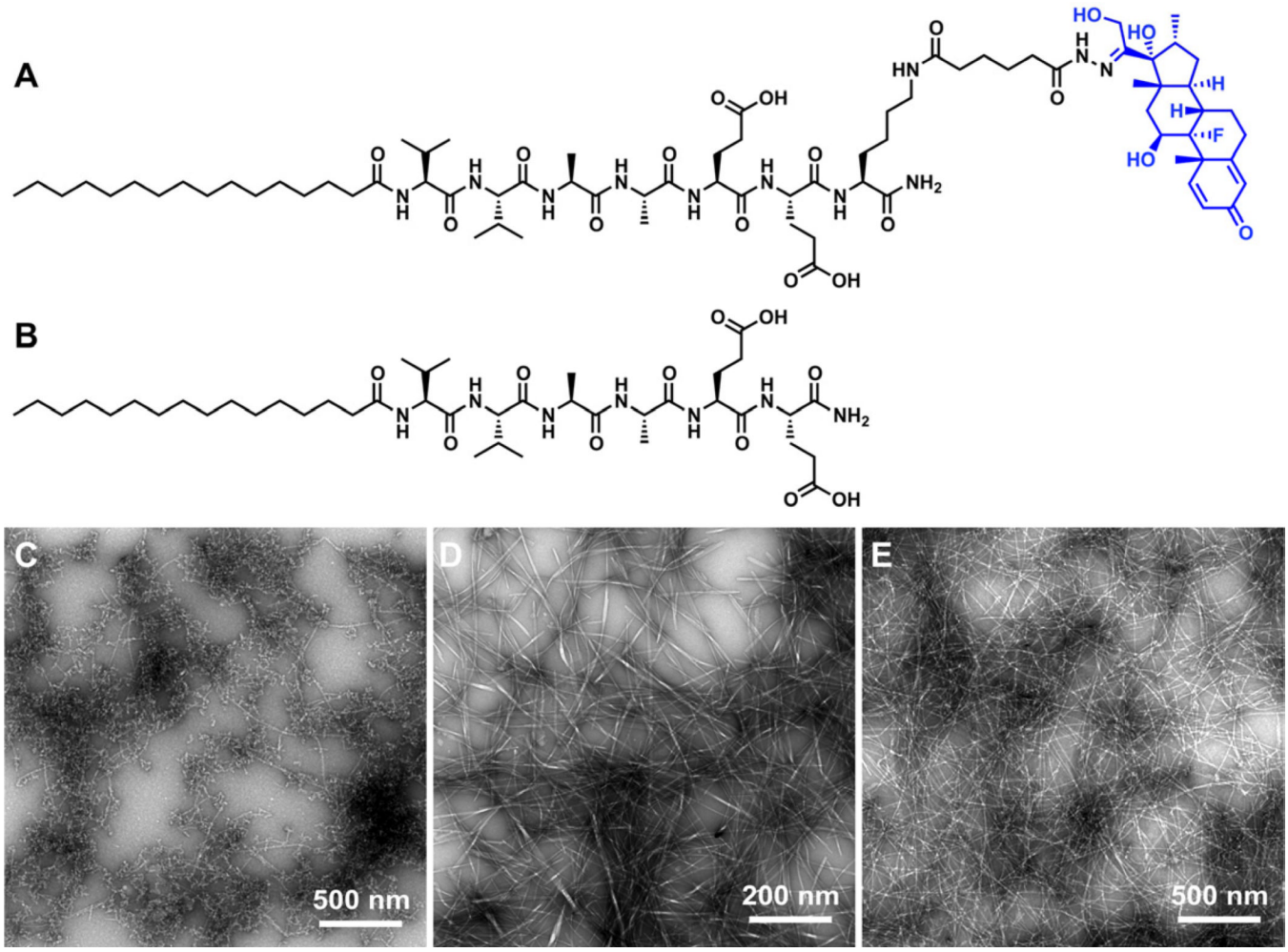

Figure 1.

The chemical structures of (**A**) the Dex-PA and (**B**) the control PA are shown. Transmission electron microscopy shows the assembled nanostructures of (**C**) pure Dex-PA (**D**) pure control PA, and (**E**) a 1:9 mixture of Dex-PA and control PA.

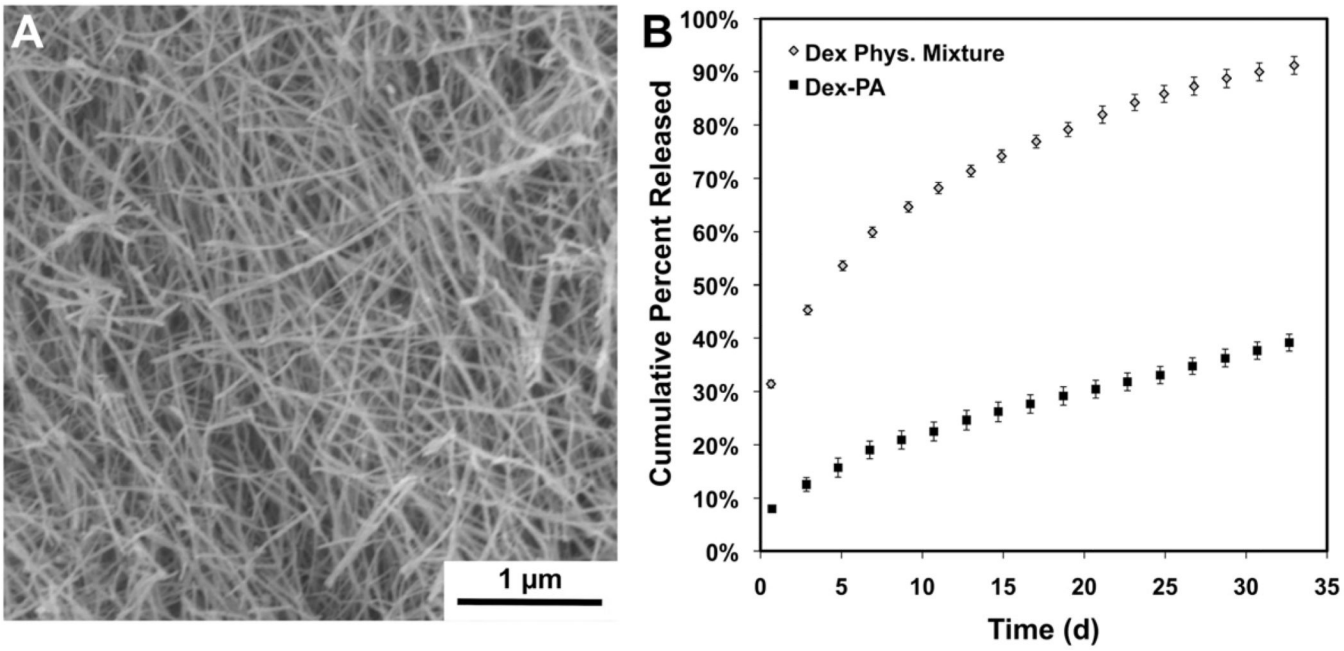

Figure 2.

(**A**) Scanning electron microscopy of a nanofiber gel prepared from a 1:9 mixture of Dex-PA and control PA under calcium screening conditions. (**B**) Cumulative release of dexamethasone from at PA nanofiber gel of this same composition over 32 days as well as release of dexamethasone that is physically mixed in a gel of the control PA over the same timeframe.

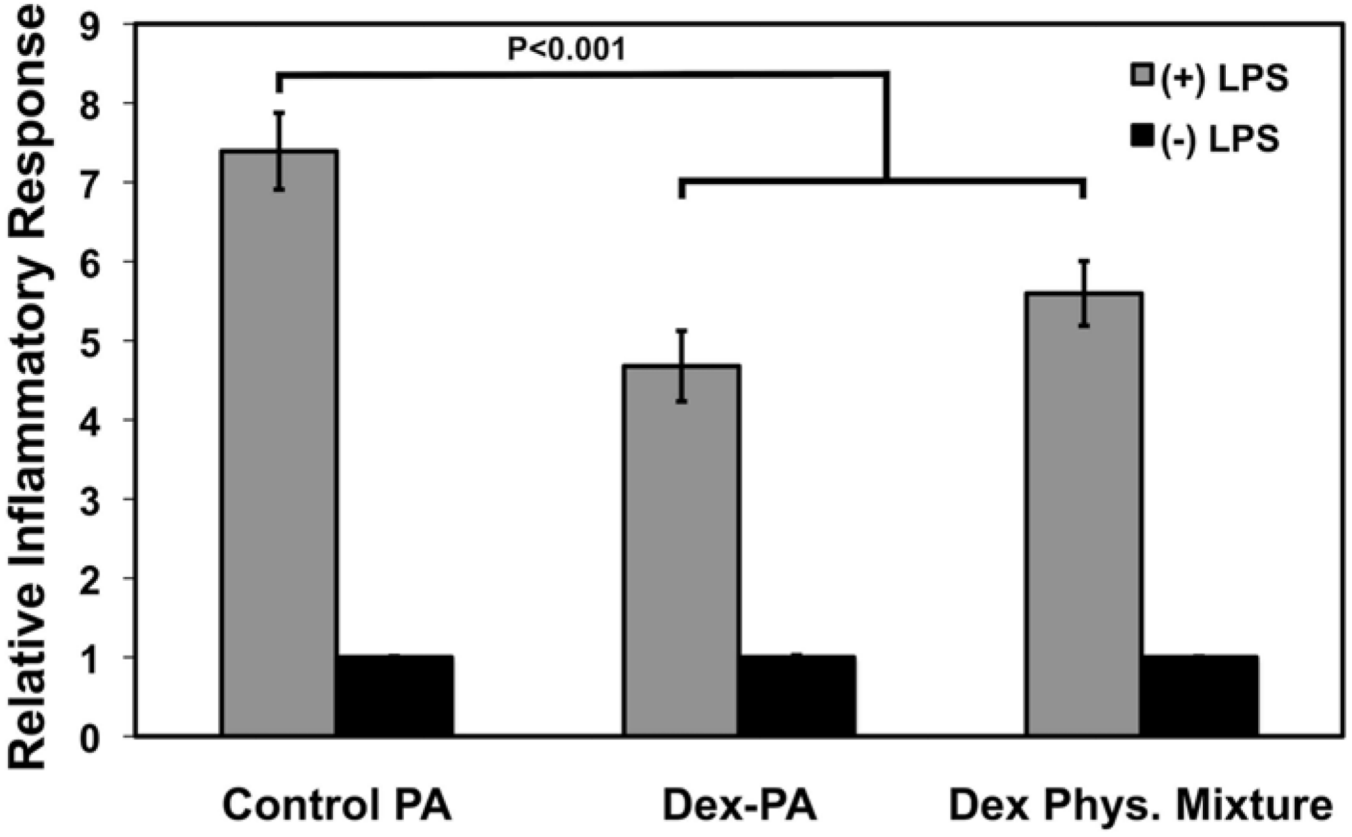

Figure 3.

Screening of an engineered THP-1 cell line for the effects of Dex-PA nanofiber gels or Dex released from a control nanofiber gel (Phys. Mixture) on NF-κB activation in response to lipopolysaccharide (LPS)-induced inflammation, as well as the same groups performed in the absence of LPS. Sampling occurred 24 hours following treatment with LPS and data is normalized to a control of media from normal cells in culture. Error bars denote standard error of the mean.

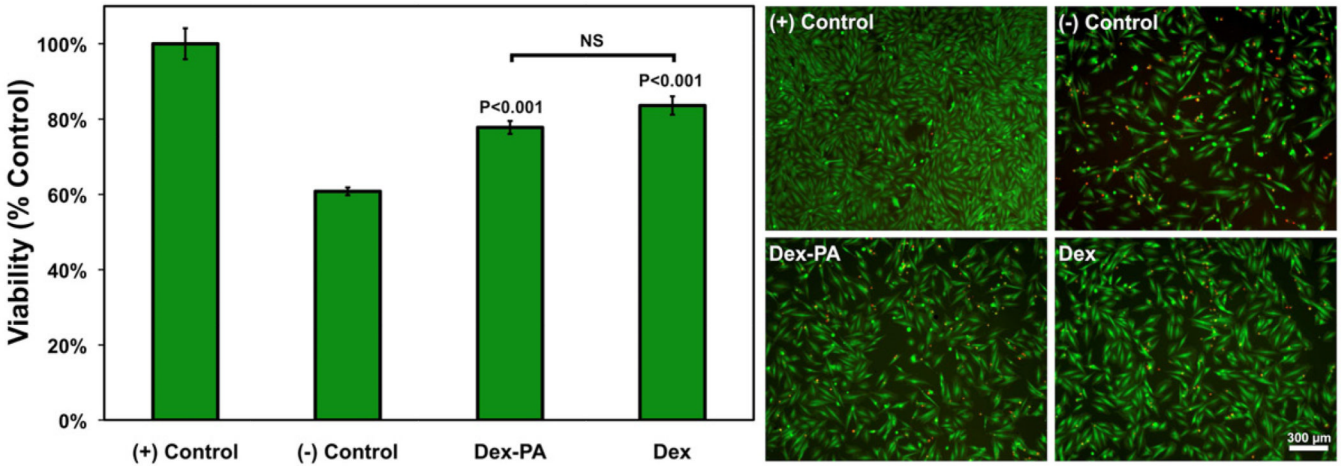

Figure 4.

Evaluation of the effects of Dex-PA and soluble Dex on the viability of an H9c2 cardiomyocyte cell line challenged with oxidative stress by 2 hours of H_2O_2 exposure, followed by treatment with Dex-PA or controls. Viability was assessed 24 hours following treatment by quantification using an MTT assay with data normalized to the untreated positive control (assumed 100%). Error bars denote standard error of the mean. Significance indicated for Dex-PA and Dex is in relation to both positive and negative controls. On the right are representative live/dead images (live=green, dead=red), also collected 24 hours following treatment to illustrate the effects of each treatment on H9c2 viability.

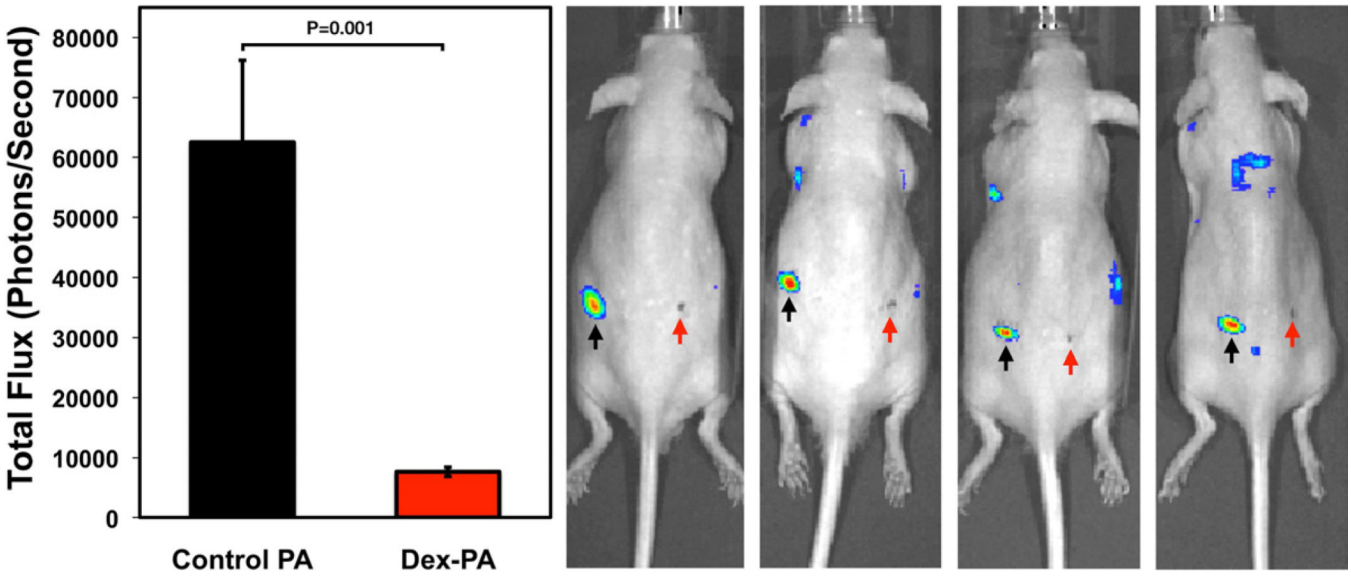

Figure 5.
Quantification and representative images of luminescence data from a luminol assay conducted on mice 3 days following subcutaneous implantation of polystyrene microparticles delivered within nanofiber gels of control PA (left site, black arrows) or a 1:9 mixture of Dex-PA and control PA Dex-PA (right site, red arrows). Error bars for quantified data denote standard error of the mean.

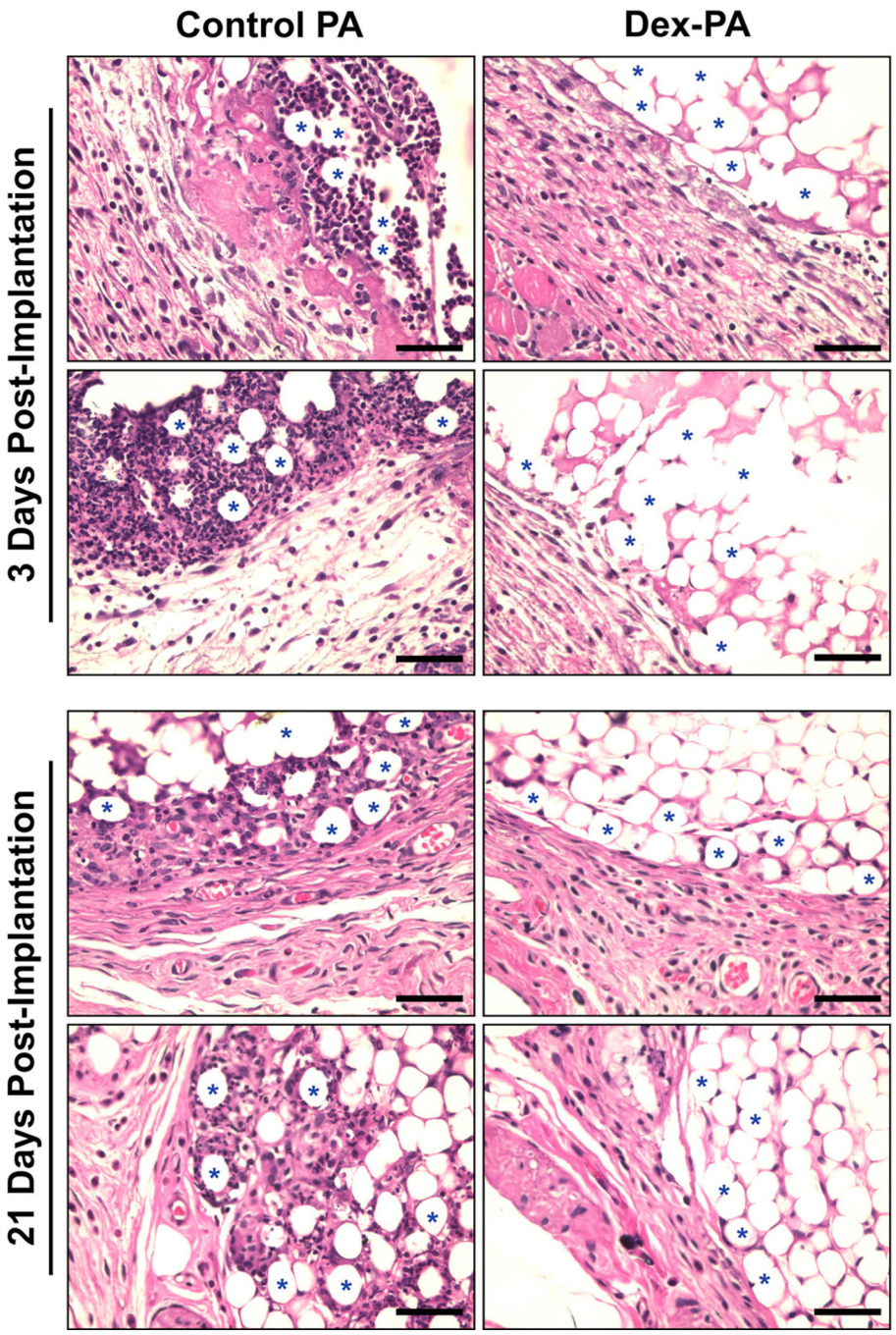

Figure 6.

Representative histology (H&E staining) of tissue harvested either 3 days (top panel) or 21 days (bottom panel) following subcutaneous implantation of polystyrene microparticles delivered within nanofiber gels of control PA (left column) or a 1:9 mixture of Dex-PA and control PA Dex-PA (right column). Blue stars denote some representative particles at the tissue/implant interface and rows correspond to images taken from the same animal. Scale bars indicate 50 μm and images were collected at 40× magnification.

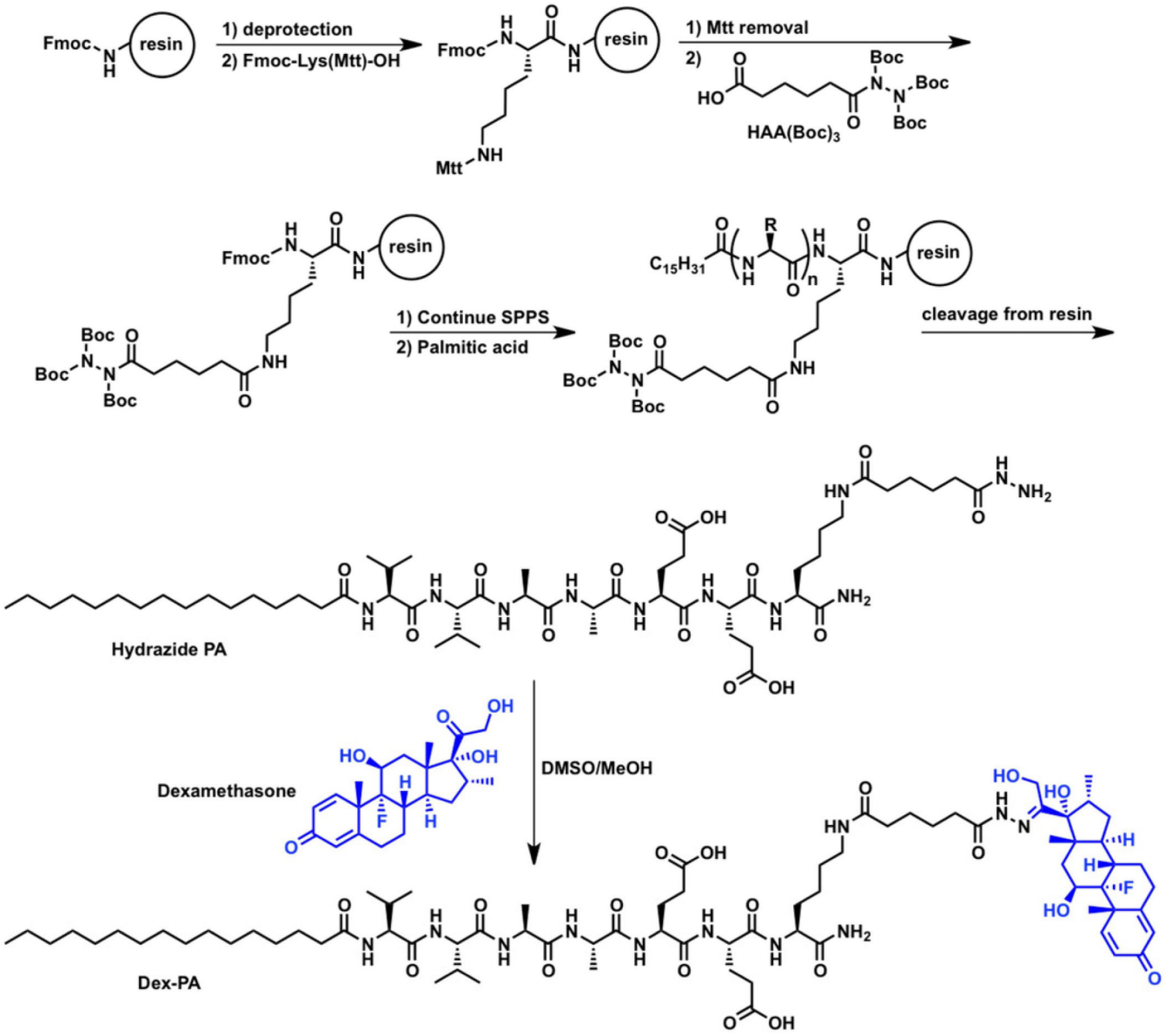

Scheme 1.

Outlined is the general procedure to orthogonally incorporate a tri-Boc-protected hydrazide ($HAA(Boc)_3$) in peptides synthesized on resin via addition to a selectively deprotected lysine residue. Standard procedures for solid phase peptide synthesis (SPPS) can be performed before and after addition of the protected hydrazide and, in the case of PA synthesis, a palmitic acid tail is coupled following stepwise peptide synthesis. Upon cleavage from the resin, a PA containing a free hydrazide is obtained which can be purified and then condensed with the ketone of dexamethasone (blue) to form the hydrazone-linked drug conjugate, termed Dex-PA.